

# Frequency Planning for a Multi-Radio 802.11s City-Wide Water Management Network

Dimitris Ntilis  
School of ECE,  
Technical Univ. of Crete  
Kounoupidiana Campus  
Chania, Greece 73100  
dntilis@hotmail.com

Panagiotis Oikonomakos  
School of ECE,  
Technical Univ. of Crete  
Kounoupidiana Campus  
Chania, Greece 73100  
panos.oikonomakos@gmail.com

Vasileios Papadakis  
Network Operation Center,  
Technical Univ. of Crete  
Kounoupidiana Campus  
Chania, Greece 73100  
ikaros.05@ict.tuc.gr

Antonios Inglezakis  
School of ECE,  
Technical Univ. of Crete  
Kounoupidiana Campus  
Chania, Greece 73100  
aigglezakis@softnet.tuc.gr

Antonis G. Dimitriou  
Dept. of ECE,  
Aristotle Univ. of Thessaloniki  
Thessaloniki, Greece 54124  
antodimi@auth.gr

Aggelos Bletsas  
School of ECE,  
Technical Univ. of Crete  
Kounoupidiana Campus  
Chania, Greece 73100  
aggelos@telecom.tuc.gr

## ABSTRACT

This work studies frequency allocation in 802.11s mesh wireless networks, employing multi-radio terminals and directive antennas. The network targets city-wide deployment and connects critical water tanks, storage reservoirs and pumping stations. The objective is to offer frequency planning with minimum remaining interference between the network terminals, under stringent and practical constraints, including a) long distances, on the order of 4 – 5 kilometers, b) radio terminals with broad beamwidths that serve multiple destinations, c) need for different frequency channels among different radio interfaces at the same terminal and d) limited number of frequency channels and transmission power. Practical centralized algorithms are provided for connectivity, conflict graph and frequency channel assignment, considering all constraints. It is shown that frequency planning under such stringent constraints is feasible.

## Keywords

Frequency allocation, interference mitigation, wireless networks.

## 1. INTRODUCTION

Deploying a city-wide, autonomous 802.11s (mesh) wireless network that connects critical water tanks, storage reservoirs and pumping stations is challenging for two main reasons: a) network planners can only install mesh network nodes at specific locations and b) links on the order of 4 – 5 kilometers must be implemented, with equivalent isotropic

Permission to make digital or hard copies of all or part of this work for personal or classroom use is granted without fee provided that copies are not made or distributed for profit or commercial advantage and that copies bear this notice and the full citation on the first page. To copy otherwise, to republish, to post on servers or to redistribute to lists, requires prior specific permission and/or a fee.

CySWater'15 April 13-16, 2015, Seattle, WA, USA  
Copyright 2015 ACM 978-1-4503-3485-3/15/04 ...\$15.00.  
<http://dx.doi.org/10.1145/2738935.2738942>



Figure 1: Overall Pilot Network Topology.

radiated power (EIRP) at each transmitter not exceeding 20 dBm, while 802.11 frequency bands in a city are unlicensed and thus, crowded. Fig. 1 offers the locations of water tanks and pumping stations that must be connected at city-wide scale in a pilot network, targeting water management.

This work utilized multiple radios at each 802.11s node, with two types of 17 dBi directive antennas: a) broad beamwidth of 120° or b) narrow beamwidth of 25° (triangle or rectangular terminals, respectively, in connectivity graph of Fig. 2 and routing tree of Fig. 3). Such approach was necessary to secure the required sensitivity of long-range links and also improve connectivity diversity with reduced cost. However, installing multiple radios on the same node (e.g.  $P_1$  has radio interfaces 1 and 2 denoted as  $P_{1-1}$  and  $P_{1-2}$ ) imposed *self-interference*, when two radios of the same node operated at the same frequency, due to electromagnetic coupling. Furthermore, the broad beamwidth imposed additional constraints on the frequency allocation problem (i.e. planning), since links served by the same antenna (radio terminal) should operate at the same frequency channel.

Interestingly, the proactive mode provided by 802.11s allows the construction of a routing tree in which the gateway

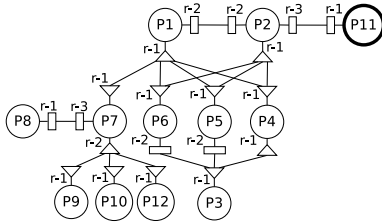


Figure 2: Connectivity Graph of the Pilot Network.

to the external internet is the “root”. The majority of the network traffic is forwarded from the mesh nodes to the gateway (through the tree structure) or vice-versa. One possible routing tree of the mesh network of Figs. 1, 2 is shown in Fig. 3.

The goal of the proposed algorithms is to find a valid frequency channel assignment that minimizes interference between the mesh nodes, while adhering to several practical constraints. First, for any given routing link, the endpoint radio interfaces must operate on the same frequency channel. Second, routing links in interference range of each other should be assigned to different frequency channels if possible. Due to the broad beamwidth antennas, meeting such constraints may not be always feasible, since a single antenna can serve several routing links. Third, radio interfaces on the same node, should operate on different channels if possible, to avoid the self-interference problem. The low number of non-overlapping channels that 802.11b offers (only channels 1, 6, 11 do not overlap), means that the last two constraints cannot always be satisfied.

For interference modeling, the concept of conflict graphs is exploited. A conflict graph  $G_c(V_c, E_c)$  is constructed from the connectivity graph  $G(V, E)$ , where each  $v \in V$  corresponds to a radio interface and each  $e \in E$  corresponds to a communication or interfering link between two radio interfaces. A conflict graph example is shown in Fig. 4. A routing graph  $G_r(V, E_r)$  is also needed, where each  $e_r \in E_r$  denotes a link alongside a routing path towards the gateway and vice-versa. A conflict graph  $G_c$  has vertices that correspond to the links in  $E_r$  and has an edge between two vertices, when the links of those vertices interfere with each other, when operating simultaneously on the same frequency channel.

The conflict graph approach followed in this work creates a vertex for each routing link between radio interfaces, instead of network nodes (as in [5]) and thus, better accommodates multi-radio terminals. Furthermore, additional prac-

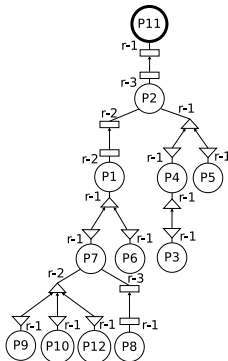


Figure 3: Routing of the Pilot Network.

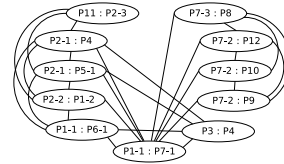


Figure 4: Conflict Graph of the Pilot Network.

tical constraints are taken into account and the proposed algorithms attempt to protect from interference long-distance (i.e. *weak*) links. From that perspective, this work departs from graph coloring approaches [3] tailored to 802.11 networks [4, 6]. The focus is on practical centralized algorithms, while distributed schemes, as in [1] are left for future work. Section 2 describes how connectivity among radio interfaces is assessed, section 3 offers the conflict graph creation algorithm, section 4 provides the frequency allocation algorithms with emphasis on multi-terminal radios and protection of weak links, and finally, section 5 discusses the results. Work is concluded in section 6.

## 2. CONNECTIVITY GRAPH ANALYSIS

Connectivity between any two radio interfaces exists when the received power is above the sensitivity of the radio interface hardware. To refer to a node’s radio interfaces, e.g. radio interface 2 of node 1, the following notation is used:  $P_{1-2}$ . When the node has only one radio interface, the node’s name is used instead, e.g.  $P_1$ . To determine if a connectivity link is a communication link or an interference link, the routing tree has to be decided first. If a connectivity link exists in the routing tree, then it will be a communication link; otherwise, it will be an interference link.

The antennas used in this work have the same maximum gain of 17dBi in each side of the link. At distance  $d_i$  between transmitter and receiver  $i$ , the signal power has experienced “one-way” propagation link loss  $L_i$ . It is assumed that the transmitter antenna is mounted at height  $h_T$  and the receiver antenna at height  $h_R$ . Taking into account the line-of-sight (LOS) path between transmitter and receiver, as well as one reflection from the ground, one-way loss,  $L_i$  can be approximated by the two-ray model loss [2]:

$$L_i = \frac{\text{received power}}{\text{transmitted power}} = \begin{cases} G_T G_R \left( \frac{\lambda}{4\pi d_i} \right)^2 & , \text{ if } d_i < d_0 \\ G_T G_R \left( \frac{h_T h_R}{d_i} \right)^2 & , \text{ if } d_i \geq d_0 \end{cases} \quad (1)$$

where  $G_T$  and  $G_R$  are the gains of the transmitter and receiver antenna respectively,  $\lambda$  is the RF carrier wavelength and  $d_0$  is given by:

$$d_0 = \frac{4\pi h_T h_R}{\lambda} \quad (2)$$

Due to the placement of antennas at high altitudes, the first case of the above formula, i.e. free space loss is used for most links, where  $d_i < d_0$ . For example, for link  $P_{2-3} \rightarrow P_{11}$  in connectivity graph of Figure 2 and carrier frequency 2.437GHz,  $P_{TX} G_T = 100\text{mW}$  (corresponding to the maximum EIRP limit),  $d_i = 2050\text{m}$ ,  $h_T = 217\text{m}$ ,  $h_R = 139.91\text{m}$ , it can be shown that  $P_{RX} = -69\text{dBm}$ , which is greater than the sensitivity  $-90\text{dBm}$  of the specific wireless cards utilized at 1 Mbps. The received power for the rest of the links is

calculated similarly and connectivity (if exists) is depicted at the respective graph of Fig. 2.

It is noted that from the sensitivity formula (at 27° C),

$$P_{RX}^{\min} = -174 \frac{\text{dBm}}{\text{Hz}} + \text{NF} + 10 \log \text{BW} + \theta, \quad (3)$$

and setting noise figure  $\text{NF} = 5\text{dB}$ , bandwidth  $\text{BW} = 11\text{MHz}$  and  $P_{RX}^{\min} = -90\text{dBm}$  (@1Mbps), the minimum signal-to-interference-and-noise ratio (SINR) threshold can be calculated on the order of  $\theta = 9\text{dB}$ , for which reliable link communication exists, i.e. when  $\text{SINR} > \theta$ . Threshold  $\theta$  will be needed at performance evaluation, subsequently.

### 3. CONFLICT GRAPH CREATION ALGORITHM

In this section, a centralized algorithm is described that creates a conflict graph  $G_c(V_c, E_c)$ , i.e. a graph where each vertex is a link and edges connect the links that could interfere each other when operating at the same frequency channel. The algorithm requires as input the connectivity graph  $G(V, E)$ , where each  $v \in V$  corresponds to a radio interface in the network and each  $e \in E$  corresponds to a communication or interference link between two of the above radio interfaces. The algorithm also needs as input the routing tree  $G_r(V, E_r)$ ,  $E_r \subseteq E$  and a radio interfaces table  $R[i, j]$ , where  $i, j \in V$  and  $R[i, j] = 1$  if  $i, j$  belong to the same node.

In the created conflict graph, each vertex corresponds to a routing link,  $l \in E_r$ , between two radio interfaces,  $i, j \in V$ . For example, in Fig. 4, the  $P_{2-1} : P_{5-1}$  conflict graph vertex exists. This means that in the original network  $P_{2-1}$  and  $P_{5-1}$  correspond to two different radio interfaces and also

the link between these two radio interfaces is a routing link. The notation  $i \in V_c$ , where  $i$  is a radio interface, means that the conflict graph vertex that contains the radio interface  $i$  is marked.

The algorithm is summarized in Algorithm 1. It starts by creating a node  $g \in V_c$  for each one of the routing links given by  $E_r$  (Lines 1,2). It connects those  $v \in V_c$  that contain a radio interface from the same node (Line 3). This is to avoid the self-interference problem when assigning channels.

The algorithm then visits each one of the newly created vertices and tries to find all other vertices that it interferes with, when operating on the same frequency channel. In lines 5-7 it finds the two radio interfaces that the visited node  $v \in V_c$  contains and adds them to a queue  $Q_1$ . Subsequently it visits every radio interface  $i \in V$  that has been added in  $Q_1$  and it finds the communication and interference links for the given radio interface. In lines 10-15 if a particular connectivity link between radio interfaces  $i, j \in V$  happens to also be a routing link, it means that if it operates simultaneously on the same channel with the link contained in the visited vertex  $v$ , there will be interference. So the algorithm finds the vertex  $u \in V_c$  that uses the  $i, j$  radio interfaces and connects it with  $v$ ,  $(v, u) \in E_c$ . The algorithm also adds the radio interface  $j$  in a second queue  $Q_2$ , for later use. On the other hand if  $(i, j) \in E$  but  $(i, j) \notin E_r$ , then it only adds the radio interface  $j$  in  $Q_2$  (Lines 8-15).

When there are no more radio interfaces in  $Q_1$ , the algorithm visits the radio interfaces that have been added in  $Q_2$  (Lines 16, 17). As before, for every radio interface  $i \in V$  that the algorithm visits, it finds its communication and interference links. If any one of those links is also a routing link (i.e.  $(i, j) \in E_r$ ), then  $(v, u) \in E_c$ , where  $u \in V_c$  the vertex that contains the  $i, j$  radio interfaces (Lines 18-21).

---

#### Algorithm 1: CONFLICT GRAPH CREATION

---

**Input:** Connectivity Graph  $G(V, E)$ , Routing Tree  $G_r(V, E_r)$ , Radio Interfaces Table  $R[i, j]$

**Output:** Conflict Graph  $G_c(V_c, E_c)$

```

1: for each edge  $l \in E_r$  do
2:   create a node  $g \in V_c$ 
3: In  $G_c$  connect the nodes where:  $i, j \in V_c, i \neq j$  and
    $R[i, j] = 1$ 
4: for each node  $v \in V_c$  do
5:   mark the two radio interfaces  $m, n$  that  $v$  contains
6:   addToQueue( $Q_1, m$ )
7:   addToQueue( $Q_1, n$ )
8:   while  $\text{size}(Q_1) > 0$  do
9:      $u = \text{removeHead}(Q_1)$ 
10:    for each  $w \in V$  do
11:      if  $(u, w) \in E$  then
12:        addToQueue( $Q_2, w$ )
13:      if  $(u, w) \in E_r$  then
14:        find  $p \in V_c$  that contains the  $u, w$  radio
        interfaces
15:        connect  $v$  with  $p$  in Conflict Graph
16:    while  $\text{size}(Q_2) > 0$  do
17:       $u = \text{removeHead}(Q_2)$ 
18:      for each  $w \in V$  do
19:        if  $(u, w) \in E_r$  then
20:          find  $p \in V_c$  that contains the  $u, w$  radio
        interfaces
21:          connect  $v$  with  $p$  in Conflict Graph

```

---



---

#### Algorithm 2: CHANNEL ASSIGNMENT BASED ON NODE DEGREE

---

**Input:** Conflict Graph  $G_c(V_c, E_c)$ , Set of Channels  $K$ , Distance between radio interfaces  $D(i, j)$

**Output:** Channel Assignment  $V_c \Rightarrow K$

```

1: while  $\exists v \in V_c$  with no channel assigned do
2:   select  $u \in V_c$  with largest node degree that has no
   channel assigned
3:    $\text{nodeDegree}(u) = -1$ 
4:   initialise  $\text{maxDist}(1, \text{numOfChannels}) = \vec{0}$ 
5:   set of available channels for  $u \triangleq C(u)$ ,  $C(u) = K$ 
6:   for each  $w \in V_c, w \neq u$  do
7:     if  $(w, u) \in E_c$  then
8:        $C(u) = C(u) - \text{channel}(w)$ 
9:       find  $D(i, j)$  between radio interfaces  $i$  and  $j$ 
   of  $w$ 
10:      if  $D(i, j) > \text{maxDist}(\text{channel}(w))$  then
11:         $\text{maxDist}(\text{channel}(w)) = D(i, j)$ 
12:    if  $C(u) \neq \emptyset$  then
13:      randomly assign channel  $c \in C(u)$  to  $u$ 
14:    else
15:      assign to  $u$  the channel  $c \in K$  that minimizes
    $\text{maxDist}$ 
16:    for each  $w \in V_c, w \neq u, w$  and  $u$  share a common
   radio interface do
17:       $\text{channel}(w) = \text{channel}(u)$ 

```

---

---

**Algorithm 3:** CHANNEL ASSIGNMENT BASED ON RADIO LINK DISTANCE

---

**Input:** Conflict Graph  $G_c(V_c, E_c)$ , Set of Channels  $K$ , Distance between radio interfaces  $D(i, j)$

**Output:** Channel Assignment  $V_c \Rightarrow K$

```
1: while  $\exists v \in V_c$  with no channel assigned do
2:   select  $u \in V_c$  with largest distance between its two
   radio interfaces  $i$  and  $j$ , that has no channel assigned
3:    $D(i, j) = -1$ 
4:   initialise  $maxDist(1, numOfChannels) = \bar{0}$ 
5:   set of available channels for  $u \triangleq C(u)$ ,  $C(u) = K$ 
6:   for each  $w \in V_c, w \neq u$  do
7:     if  $(w, u) \in E_c$  then
8:        $C(u) = C(u) - channel(w)$ 
9:       find  $D(i, j)$  between radio interfaces  $i$  and  $j$ 
   of  $w$ 
10:      if  $D(i, j) > maxDist(channel(w))$  then
11:         $maxDist(channel(w)) = D(i, j)$ 
12:      if  $C(u) \neq \emptyset$  then
13:        assign to  $u$  the channel  $c \in C(u)$  that is the most
        used in its 2-hop neighborhood
14:      else
15:        assign to  $u$  the channel  $c \in K$  that minimizes
         $maxDist$ 
16:      for each  $w \in V_c, w \neq u, w$  and  $u$  share a common
        radio interface do
17:         $channel(w) = channel(u)$ 
```

---

## 4. CHANNEL ASSIGNMENT ALGORITHMS

Two heuristic centralized algorithms are proposed that solve the frequency allocation problem, based on vertex coloring on the created conflict graphs.

### 4.1 Channel Assignment Based on Node Degree

As input, the channel assignment algorithm needs a valid conflict graph  $G_c(V_c, E_c)$ , a set of frequency channels  $K$  and the Euclidean distance  $D$ , between any two radio interfaces  $i, j$ , where  $(i, j) \in E$ . The latter is important in order to protect the weaker links of the network, i.e. links with distance between radio interfaces greater than 4 kilometers, when assigning frequency channels. In the 2.4 GHz band, there are only 3 non overlapping channels that can be used simultaneously without causing interference. So the set  $K$  contains only three channels denoted (for simplicity) as channel 1, 2 and 3, corresponding to 802.11b frequency channels 1, 6 and 11, respectively.

In order to protect the weaker links (i.e. those with large distance), the  $maxDist$  vector is utilized; this vector is initialized as a null vector and it is used when there are no interference free channel assignments for a particular conflict graph vertex. The  $maxDist$  vector will lead to an assignment that causes interference with conflict graph vertices that have smaller distance between the radio interfaces, thus protecting the weak links.

Algorithm 2 starts by visiting the vertex  $v \in V_c$  with the largest node degree that has no channel assigned (Lines 1-3). Based on the conflict graph, the algorithm then finds the interfering vertices  $u_i \in V_c$  with  $v$ . The channels used by  $u_i$  are marked as unavailable for  $v$  (Lines 6-8). For those  $u_i$  that

can interfere with  $v$ , the algorithm also marks the distance of the radio link so it can protect the link with the largest distance (Lines 9-11). Subsequently, the algorithm checks if there exist available channels for the vertex  $v$ . If there exist, it will randomly assign one of the available channels to  $v$  and if not, it will assign to  $v$  the channel that is used by the links with the smallest distance between the radio interfaces (Lines 12-15).

In the final stage, the algorithm finds all other  $p \in V_c$  that share a common radio interface with  $p$  and assigns them the same channel (Lines 16-17). This is due to the fact that it must be ensured that the algorithm assigns only one channel to each radio interface.

### 4.2 Channel Assignment Based on Radio Link Distance

This is similar to the Algorithm 2 with one key difference; the algorithm visits the vertices of the conflict graph, based on the largest distance of a routing link (which is equivalent with the vertex  $v \in V_c$  that contains the radio interfaces that form the link) (Lines 1-3), instead of the node degree. The next steps are exactly the same as in Algorithm 2.

The last difference between Algorithm 3 and Algorithm 2 occurs at line 13. If there is an available channel for assignment to vertex  $v \in V$ , this algorithm will select the available one which is mostly used in the 2-hop neighborhood of  $v$ . The intuition behind this decision is that if a vertex randomly selected a not so frequently used channel, it could prevent another vertex to choose the same channel. Due to the frequency usage of the said channel, the latter vertex may not have another available choice for channel selection without interference. Such technique was found useful in the numerical results for this algorithm, in order to reduce the remaining interference. However, such modification was not necessary for Algorithm 2, as observed during tests for both algorithms.

## 5. SIMULATION RESULTS

Frequency channel allocation is evaluated in terms of remaining interference. The frequency allocation algorithms are tested in two different network scenarios; the first one is a subset of the pilot testbed and consists of 7 nodes (Fig. 5 (left)) and the second is the pilot testbed and consists of 12 nodes (Fig. 2).

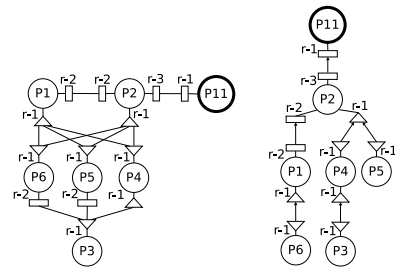


Figure 5: Communication Link Graph of the Small Network Topology (left). Routing of the Small Network (right).

One possible routing tree for the small and the pilot network, is shown in Fig. 5 (right) and Fig. 3, respectively. Based on those routing trees, the conflict graphs are constructed using the aforementioned Algorithm 1. The results

are shown in Fig. 6 and Fig. 4 for the small and the large (pilot) network, respectively.

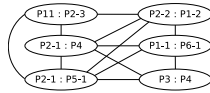


Figure 6: Conflict Graph of the Small Network.

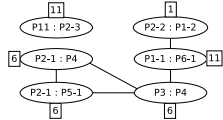


Figure 7: Remaining Interference after Channel Assignment of Algorithm 2 on the Small Network.

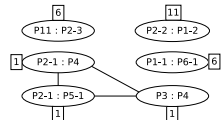


Figure 8: Remaining Interference after Channel Assignment of Algorithm 3 on the Small Network.

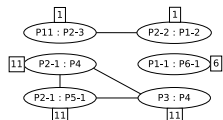


Figure 9: Remaining Interference after Channel Assignment of Tabu Algorithm on the Small Network.

The channel allocation for the small network of Algorithm 2, Algorithm 3 and the Tabu [5] is shown in Fig. 7, Fig. 8 and Fig. 9, respectively. Multi-radio node  $P_2$  is assigned different channels in the first two algorithms, however, remaining 2-hop interference (imposing hidden-node terminal) is not addressed with the 3rd algorithm. The rest of remaining interference is due to the directional antennas, serving more than one link and could be alleviated only with time-based medium access control. We should note here that the Tabu based algorithm does not always result in assignments with more interference than those created by the proposed algorithms; due to its continuous randomized selection of channels, the Tabu algorithm may result with the same remaining interference as our algorithms, but not better, for the studied network cases. The resulting frequency allocation network for the above 3 algorithms in the small network, is shown in Fig. 10 (left), Fig. 10 (right) and Fig. 11.

Channel allocation for the pilot network of Algorithm 2, Algorithm 3 and Tabu is shown in Fig. 12, Fig. 13 and Fig. 14, respectively. All three algorithms offer the same interfering links, although different iterations of the Tabu based algorithm may result with more interfering links. Both multi-radio nodes  $P_2$  and  $P_7$  are assigned different frequency channels among their radio interfaces, in all cases. As with the small network, the remaining interference is due to the fact that the same antenna serves more than one links and the connected radio is constrained to use the same frequency channel. The resulting network planning with frequency allocation for the above 3 algorithms is shown in Fig. 15 (left), Fig. 15 (right) and Fig. 16. The frequency allocation results are very similar in all cases. That may seem surprising

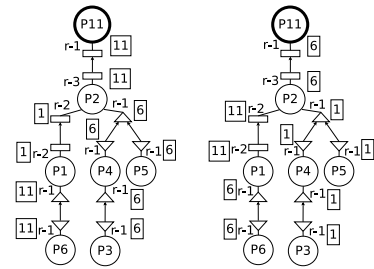


Figure 10: Routing with the Channel Assignment of Algorithm 2 (left) and Algorithm 3 (right) on the Small Network.

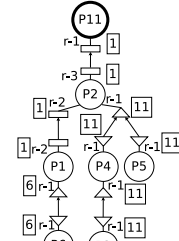


Figure 11: Routing with the Channel Assignment of Tabu Algorithm on the Small Network.

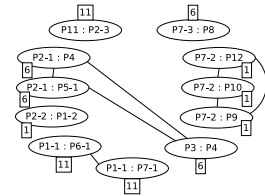


Figure 12: Remaining Interference after Channel Assignment of Algorithm 2 on the Pilot Network.

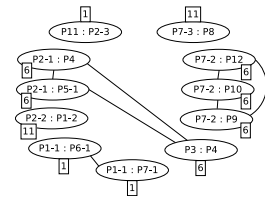


Figure 13: Remaining Interference after Channel Assignment of Algorithm 3 on the Pilot Network.

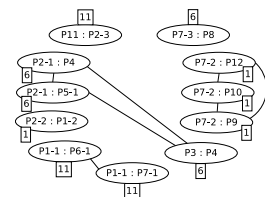


Figure 14: Remaining Interference after Channel Assignment of Tabu Algorithm on the Pilot Network.

and is attributed to the multiple constraints imposed on the problem, including operation at a specific frequency channel per radio card (even when that card serves multiple links through a broad beamwidth antenna) and inability to place antennas in specific places. Nevertheless, broad beamwidth antennas increase network robustness through path diversity and also decrease installation cost (since path diversity is achieved with one radio).

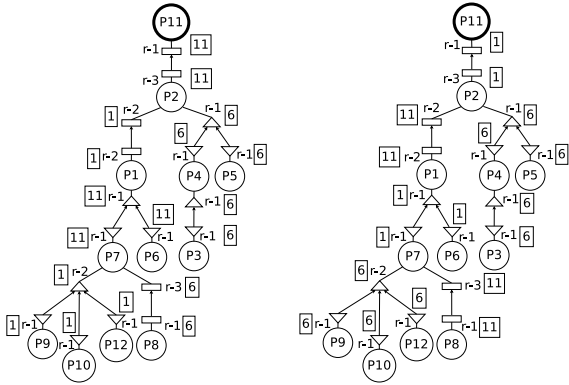


Figure 15: Routing with the Channel Assignment of Algorithm 2 (left) and Algorithm 3 (right) on the Pilot Network.

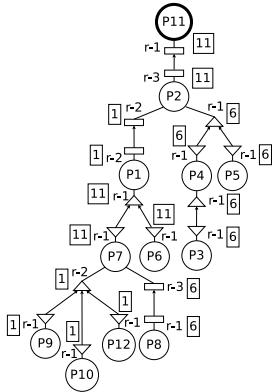


Figure 16: Routing with the Channel Assignment of Tabu Algorithm on the Pilot Network.

## 5.1 Bottleneck and Outage Analysis

In the pilot (large) network of Fig. 3 there is always radio interface  $P_{7-2}$  receiving from 3 different radio terminals  $P_9, P_{10}, P_{12}$ , for all three frequency allocation algorithms. Therefore, one possible way to mitigate interference among the three links is through time-sharing (e.g. CSMA) of the 1 Mbps capacity; in that case, the end-2-end bottleneck bandwidth will be dominated by the above sharing, since all other radios in the network serve no more than two links.

Similar results hold for the smaller network of Fig. 5 (right), where time sharing among at most 2 links is required in order to mitigate remaining interference. Algorithm 2 and Algorithm 3 produce the same results regarding remaining interference after frequency channel assignment (Figs 7, 8). In the Tabu-based frequency assignment (Fig. 9) there are two radio interfaces of a node in the same frequency channel ( $P_{2-2}$  and  $P_{2-3}$ ), which may create self-interference between those radio interfaces.

For worst-case analysis, one could calculate the outage probability when interference cannot be mitigated. Taking into account average received power for each receiver as calculated in the connectivity graph section and assuming Rayleigh fading (which may not be appropriate for the considered setup but could offer a baseline metric), outage

probability for  $J$  interfering radios is given by:

$$\Pr(\text{SINR}_{\text{RX}} \leq \theta) \triangleq \Pr\left(\frac{g_{\text{RX}} P_{\text{RX}}}{N_0 + \sum_{j=1}^J g_j P_j} < \theta\right) \quad (4)$$

$$= 1 - e^{-\frac{\lambda_0 \theta N_0}{P_0}} \prod_{j=1}^J \frac{1}{1 + \frac{\lambda_0 P_j}{\lambda_j P_{\text{RX}} \theta}}, \quad (5)$$

where  $\{g_j\}$  is exponentially distributed with unit parameter ( $\lambda_0 = \lambda_j = 1$ ),  $\theta$  is given from Eq. (3) and  $N_0$  is receiver's thermal noise power. For example, the outage probability for link  $P_9 \rightarrow P_{7-2}$ , assuming  $P_{10}$  and  $P_{12}$  also transmit at the same frequency channel, is calculated equal to 85.3%. Similar calculations can be easily conducted for all links with remaining interference (and will be reported elsewhere).

## 6. CONCLUSIONS

Overall, this work offers a concrete planning strategy for a low-cost, frequency-agile, city-wide, 802.11s, multi-terminal wireless network, targeting water monitoring and management applications. Thus, innovative cyber-physical system (CPS)-based sensing and actuation technologies could be deployed on top of the proposed communication and networking technology.

## 7. ACKNOWLEDGMENTS

This work was supported by the SYN11-6-925 AquaNet project, which is executed within the framework of the "Cooperation 2011" program of the Greek General Secretariat for Research & Technology (GSRT), funded through European Union and national funds. The authors thank E. Kampianakis and the research personnel of the Telecommunication Systems Research Institute (Technical University of Crete, Greece) for their assistance in conducting this research.

## 8. REFERENCES

- [1] P. N. Alevizos, E. Vlachos, and A. Bletsas. Factor graph-based distributed frequency allocation in wireless sensor networks. In *Proc. IEEE GLOBECOM*, Austin, TX, December 2014.
- [2] W. Jakes. *Microwave mobile communications*. IEEE Press classic reissue. IEEE Press, 1974.
- [3] D. Karger, R. Motwani, and M. Sudan. Approximate graph coloring by semidefinite programming. *J. ACM*, 45(2):246–265, March 1998.
- [4] J. Riihijarvi, M. Petrova, and P. Mahonen. Frequency allocation for WLANs using graph colouring techniques. In *Proc. IEEE WONS*, pages 216–222, Washington, DC, January 2005.
- [5] A. P. Subramanian, H. Gupta, S. R. Das, and J. Cao. Minimum interference channel assignment in multiradio wireless mesh networks. *IEEE Trans. Mobile Comput.*, 7(12):1459–1473, December 2008.
- [6] E. G. Villegas, R. V. Ferré, and J. P. Aspas. Implementation of a distributed dynamic channel assignment mechanism for IEEE 802.11 networks. In *Proc. IEEE PIMRC*, pages 1458–1462, Berlin, Germany, September 2005.